L1 AND L2 NORM DEPTH-REGULARIZED ESTIMATION OF THE ACOUSTIC ATTENUATION AND BACKSCATTER COEFFICIENTS USING DYNAMIC PROGRAMMING

Zara Vajihi[⋆]*, Ivan Rosado-Mendez*[†]*,Timothy J. Hall*[‡]*, and Hassan Rivaz*[⋆]

[⋆] Department of Electrical and Computer Engineering, Concordia University, Montreal, CA
[†] Instituto de Fisica, Universidad Nacional Autonoma de Mexico, Mexico City, MEX
[‡] Department of Medical Physics, University of Wisconsin-Madison, Madison, WI, USA

ABSTRACT

Quantitative Ultrasound (QUS) techniques aim at quantifying backscatter tissue properties to aid in disease diagnosis and treatment monitoring. These techniques rely on accurately compensating for attenuation from intervening tissues. Various methods have been proposed to this end, one of which is based on a Dynamic Programming (DP) approach with a Least Squares (LSq) based cost function and L2 norm regularization to simultaneously estimate attenuation and parameters from the backscatter coefficient. As a way to improve the accuracy and precision of this DP method, we propose to use L1 norm instead of L2 norm as the regularization term in our cost function and optimize the function using DP. Our results show that DP with L1 regularization substantially reduces bias of attenuation and backscatter parameters compared to DP with L2 norm. Furthermore, we employ DP to estimate the QUS parameters of two new phantoms with large scatterer size and compare the results LSq, L2 norm DP and L1 norm DP. Our results show that L1 norm DP outperforms L2 norm DP, which itself outperforms LSq.

Index Terms— Quantitative ultrasound, Backscatter, Attenuation, Dynamic Programming, L1 norm regularization

1. INTRODUCTION

Ultrasound is recognized as a noninvasive, real-time, and low-cost imaging modality with broad clinical applications both in diagnosing and treating stages. As the name describes, the functionality of this modality is based on the detection of backscattered acoustic waves within tissue in the megahertz (ultrasound) frequency range. Despite the information-rich frequency content of these radiofrequency (RF) echo signals, the conventional utilization of ultrasound is a grayscale image, titled B-mode image, which is exclusively the envelope of the amplitude of the ultrasound wave. Quantitative Ultrasound (QUS) methods provide estimates of attenuation and backscattering properties of the tissue by processing the raw RF signals. Identifying such quantitative acoustic properties of tissue is of paramount importance in classification of pathology.

Characterization and classification of thyroid nodules [1] and kidneys [2], diagnosis of fatty liver [3], and detection of preterm birth risk [4] are a few of many clinical applications of QUS. However, accurately estimating QUS coefficients is still the challenge of many studies such as [5] and [6]. In order to address this issue, we recently proposed a Dynamic Programming (DP) algorithm, [7] which is based on a Least Squares (LSq) method with L2 norm depth-regularization assuming piece-wise continuous tissue properties. This novel method substantially reduced the bias and variance of estimation compared to previous work with LSq [8]. Nevertheless, the accuracy of the predicted values at the discontinuities of acoustic properties in inhomogeneous tissues could still be improved.

Here we build upon our recent work [7] in two ways. First, we propose L1 norm regularization instead of L2 norm for DP optimization to improve parameter estimate accuracy at tissue boundaries. Second, we estimate backscattering and attenuation coefficients of a tissue-mimicking phantom with marked difference in the frequency dependence of backscatter, which is related to the size of diffuse scatterers contributing to the ultrasound echo signal.

2. METHODS

Quantitative ultrasound often aims at estimating attenuation and backscattering, and parameters derived from them. The total attenuation along an RF line is usually modeled as:

$$A(f,z) = exp(-4\alpha f z) \tag{1}$$

where A is the total attenuation corresponding to frequency f and depth z, and α is the effective attenuation coefficient versus frequency (i.e., the average attenuation from intervening tissues). Backscattering is often parameterized with the following power-law equation:

$$B(f) = bf^n \tag{2}$$

where b is a constant coefficient and n represents the frequency dependence. Our goal is to find the values of α, b and n from Eq. 1 and 2.

Let $S_s(f,z)$ and $S_r(f,z)$ be, respectively, the echo signal power spectra from the sample and reference phantoms

obtained using the same ultrasound transducer and the same imaging settings (i.e. frequency, focal properties, etc). Taking the ratio of the two spectra eliminates any dependence on the imaging setting, leaving only attenuation and backscatter-dependent terms:

$$RS(f,z) = \frac{S_s(f,z)}{S_r(f,z)} = \frac{B_s(f)}{B_r(f)} . \frac{A_s(f,z)}{A_r(f,z)} = \frac{b_s f^{n_s}}{b_r f^{n_r}} exp\{-4(\alpha_s - \alpha_r) f.z\} \quad (3)$$

where the subscripts s and r refer to the sample and the reference phantoms, respectively. After taking the natural logarithm and some manipulation, we have:

$$X(f,z) = b + n \ln f - 4\alpha f z \quad (4)$$

where X is the natural logarithm of RS which is known from the experimental data, $b = \ln(b_s/b_r)$, $n = n_s - n_r$, and $\alpha = \alpha_s - \alpha_r$. The goal is to estimate α, b and n, which reveal quantitative properties of the sample. We now show how these parameters can be estimated using DP.

2.1. Dynamic Programming (DP)

We proposed DP [7] to solve for α, b and n using the following cost function:

$$C = D + R \quad (5)$$

where D and R were respectively the data and regularization terms. The data term was defined as a least squares cost function based on Eq. (4) as:

$$D = \sum_{i=1}^{K} (X(f_i,z) - b - n \ln f_i + 4\alpha f_i z)^2 \quad (6)$$

and R was set to L2 norm regularization:

$$R = w_\alpha(\alpha_j - \alpha_{j-1})^2 + w_b(b_j - b_{j-1})^2 + w_n(n_j - n_{j-1})^2 \quad (7)$$

with subscripts j and $j-1$ referring to axial positions at the current and previous rows, and w_α, w_b, and w_n are the regularization weights for each unknown. The Least Squares (LSq) proposed by [8] considered only the minimization of eq. 6.

In this work, we propose to use the L1 norm as follows:

$$R = w_\alpha|\alpha_j - \alpha_{j-1}| + w_b|b_j - b_{j-1}| + w_n|n_j - n_{j-1}| \quad (8)$$

Let $\mathbf{u}$ encapsulates the unknowns as follows:

$$\mathbf{u} = [\alpha, b, n] \quad (9)$$

To find the global optimum of this cost function, we use the efficient DP framework, and formulate the following recursive cost function:

$$C(j, \mathbf{u}_j) = \min_{\mathbf{u}} \{C(j-1, \mathbf{u}_{j-1}) + R(\mathbf{u}_{j-1}, \mathbf{u})\} + D \quad (10)$$

The minimization is performed on three unknowns $\mathbf{u}$ at each location. The term $C(j-1, \mathbf{u}_{j-1})$ indicates that we need to take into account value of the cost functions from the previous axial row. So, in order to find the $C(j, \mathbf{u}_j)$ value at the current axial position, we have to evaluate R at α, b, and n and add it to the C matrix of the previous axial row. Then, we must find the minimum value of this summation, add the data value D to it, and finally store it in the corresponding element of the cost function matrix.

In the process of finding the minimum value, we also have to store the values of $\mathbf{u}_j$ for which this minimization occurs (technically known as memoization). These locations are stored in M, a 4D matrix with the same size as C.

The DP cost function must be calculated for every axial row. After that, starting from the last axial row, we trace back the minimum points to the first row using the memoization matrix M.

3. DATA ACQUISITION

Three pairs of tissue mimicking phantoms, each pair including a sample and a reference, were used to compare the performance of LSq, DP L1 and DP L2. The first pair consisted of homogeneous blocks of agarose-based gels. The sample and reference contained 75–90 μm diameter and 5–40 μm diameter glass beads, respectively, creating backscatter coefficients with different frequency dependence. The sample of the second pair was composed of three layers of an emulsion of ultrafiltered milk and water-based gelatin with 5–43 μm diameter glass beads as sources of scattering (3000E, Potters Industries, Valley Forge, Pennsylvania), where the central layer was more attenuating than the outer two. Finally the last sample had three layers of uniform attenuation in which the central layer was of 6 dB higher backscatter than the other two layers. The reference of two layered phantoms was the top layer of each scanned from its side. All phantoms were scanned with a Siemens Acuson S2000 using linear array transducers as described in our previous paper[7].

Both LSq and DP were implemented on the RF data frames using custom-built MATLAB routines. Echo-signal power spectra were computed at different axial and lateral locations by raster-scanning a $4\times4\text{mm}^2$ spectral estimation window with a 85% overlap ratio and using a multitaper approach with NW=3 [9]. This approach produced a power spectrum array with 74 rows and 40 columns for the homogeneous phantom and an array with 108 rows and 86 columns for the layered phantoms, which correspond to different axial and lateral locations, respectively. Each cell contained a vector of normalized power spectrum estimates. The LSq and DP estimators were fed with the normalized power spectra in the frequency range from 3.7 MHz to 7 MHz corresponding to the spectral band with power content at least 10dB above the noise floor measured at 15MHz.

We applied L1 and L2 norm DP, as well as LSq to four different lateral positions from 10 different frames of RF data,

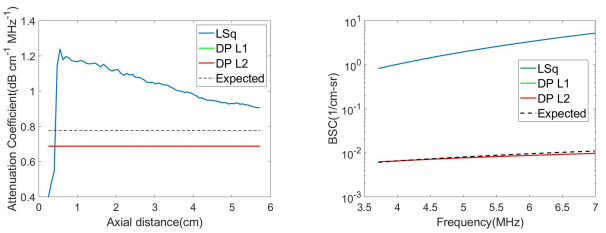

(a) Attenuation Coefficient α of homogeneous phantom (b) Backscatter Coefficients of homogeneous phantom

Fig. 1. LSq, DP L1 and DP L2 estimation of (a) attenuation coefficient and (b) backscatter coefficients of Eq. 2 in the homogeneous phantom with. DP L2 (red) collapsed on DP L1 (green) as both regularization norms result in same estimations for constant coefficients.

Table 1. The DP regularization weights for each variable.

	DP L1			DP L2		
	w_α	w_b	w_n	w_α	w_b	w_n
UniformPh	10^8	10^8	10^8	10^8	10^8	10^8
UniformBSC	10^3	100	100	10^6	10^3	10^3
UniformAtt	10^6	50	50	$5 * 10^6$	10	10

i.e 40 sample positions in total for each phantom. The weight of the regularization term in DP was set to a fixed value given in Table 1 in all 40 sample positions of the homogeneous phantom (UniformPh), the layered phantom with uniform backscatter coefficients (UniformBSC) and the layered phantom with uniform attenuation (UniformAtt). The weights for L2 regularization are the same wights used in [7] and those for L1 are determined similarly based on the thresholding method represented in [7] too. The following search ranges were used for both LSq and DP:

$$\alpha_{sMin} - 0.5 \leqslant \alpha \leqslant \alpha_{sMax} + 0.5$$

$$10^{-1} b_{sMin} \leqslant b \leqslant 10^{1} b_{sMax}$$

$$n_{sMin} - 2 \leqslant n \leqslant n_{sMax} + 2$$

where α_{sMin}, b_{sMin}, and n_{sMin} refer to the minima of the ground truth values in three layers of the layered phantoms and the ground truth values for the homogeneous phantoms for the coefficient α, b, and n, respectively, and α_{sMax}, b_{sMax}, and n_{sMax} correspondingly refer to the maxima of the ground truth values in three layers of the layered phantoms for the coefficient α, b, and n.

4. RESULTS

Figs. 1-3(a) show the DP L1 (green), DP L2 (red) and the LSq (blue) estimates of attenuation vs axial distance for the homogeneous sample of large scatterers, the layered phantom with constant backscatter, and the layered phantom with constant attenuation, respectively. Fig.1 (b) and Figs. 2 and 3 (b)–(d) show the reconstructed sample BSC from estimates of parameters b_s and n_s. Black dashed lines indicates expected values. DP L1 and L2 substantially outperforms LSq in estimation of all three parameters. In Fig.1, the DP L2 (red) collapsed on DP L1 (green) plot as both regularization norms result in same estimations for constant coefficients.

Table 2. The STD and bias in the Layered Phantom with Uniform Attenuation. In each layer, the smallest values are highlighted in bold font.

	Layer 1		Layer 2		Layer 3	
	DP L1	DP L2	DP L1	DP L2	DP L1	DP L2
STD						
α (dB/cm-MHz)	**2.24e-16**	3.92e-16	**1.15e-16**	2.30e-16	**1.14e-16**	2.84e-16
b (1/cm-sr-MHz^n)	**3.86e-09**	3.52e-07	**2.92e-07**	8.75e-07	**8.08e-09**	4.46e-07
n	**0.0584**	0.0856	0.1392	**0.0500**	0.2666	**0.1860**
Bias						
α (dB/cm-MHz)	**0.0393**	0.0547	**0.0409**	0.0562	**0.0454**	0.0608
b (1/cm-sr-MHz^n)	**5.61e-07**	6.44e-07	2.25e-06	**1.18e-06**	**1.39e-06**	2.21e-06
n	**0.4489**	0.4599	0.3006	**0.0647**	**0.2143**	0.4281

As demonstrated in the figures, DP L1 outperforms DP L2 in terms of reducing bias error in layered phantoms. Except for the bias of estimated value for backscatter coefficients, other results by DP L1 were improved compared to DP L2 and LSq.

The quantitative comparison in terms of bias and STD for DP L1 and DP L2 are given in Table 2 and Table 3 which describe the figures better. Although DP L2 estimates backscatter coefficients individually better than DP L1, the constructed backscatters for DP L1 fit better to the constructed backscatter with expected values.

5. CONCLUSIONS

We proposed employing Dynamic Programming (DP) with an L1 norm regularization term to estimate the backscatter and attenuation coefficients of radiofrequency signals obtained from the ultrasound machine. The L1 norm regularization improved the accuracy of the estimation mainly in the discontinuities of the layered phantoms. This substantially reduced the bias in the attenuation estimation of layered phantoms and slightly improved the accuracy of the backscatter estimations. We also applied the algorithm to a uniform phantom with n markedly different from the reference and compared the results of L1 and L2 norm to LSq. Because of the continuity of the coefficients along the phantom, L1 and L2 result in the same estimation which is profoundly more precise than LSq. We are currently testing the performance of both L1 and L2 regularization in DP when there are sources of coherent scattering present, such as strong scatterers or specular tissue boundaries.

6. REFERENCES

[1] A. Coila et al, "In vivo attenuation estimation in human thyroid nodules using the regularized spectral log differ-

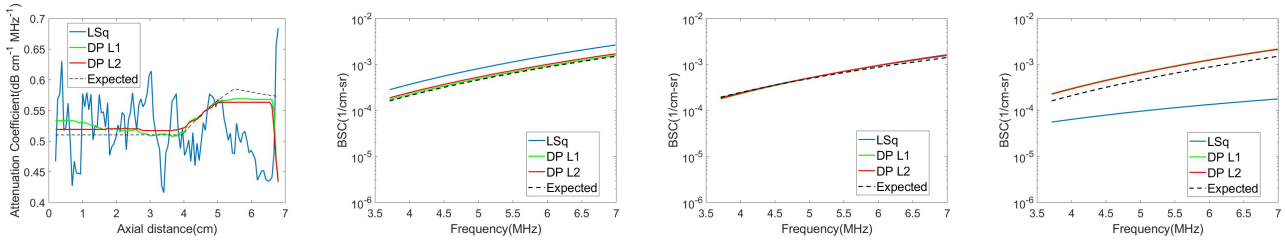

(a) Attenuation Coefficient α (b) Backscatter Coefficients of Layer1 (c) Backscatter Coefficients of Layer2 (d) Backscatter Coefficients of Layer3

Fig. 2. LSq, DP L1 and DP L2 estimation of (a) attenuation coefficient and (b–d) backscatter coefficients of Eq. 2 in the three-layered phantom with uniform backscatter coefficients for layer 1, 2, and 3, respectively.

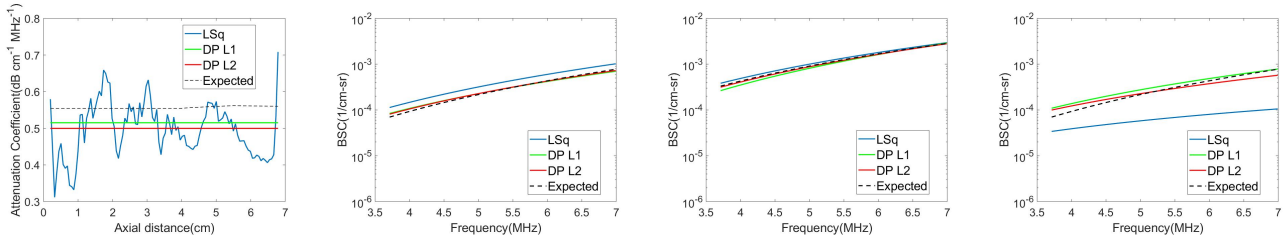

(a) Attenuation Coefficient α (b) Backscatter Coefficients of Layer1 (c) Backscatter Coefficients of Layer2 (d) Backscatter Coefficients of Layer3

Fig. 3. LSq, DP L1 and DP L2 estimation of (a) attenuation coefficient and (b–d) backscatter coefficients of Eq. 2 in the three-layered phantom with uniform attenuation coefficients for layer 1, 2, and 3, respectively.

Table 3. The STD and bias in the Layered Phantom with Uniform Backscatter. In each layer, the smallest values are highlighted in bold font.

	Layer 1		Layer 2		Layer 3	
	DP L1	DP L2	DP L1	DP L2	DP L1	DP L2
STD						
α (dB/cm-MHz)	0.0086	**0.0012**	0.0137	**0.0102**	0.0048	**0.0037**
b (1/cm-sr-MHz^n)	**4.70e-09**	5.75e-09	6.55e-09	**2.71e-09**	2.49e-08	**9.65e-09**
n	**0.0172**	0.0203	**0.0036**	0.0127	0.0076	**0.0071**
Bias						
α (dB/cm-MHz)	0.0107	**0.0087**	**0.0032**	0.0050	**0.0088**	0.0125
b (1/cm-sr-MHz^n)	**1.86e-07**	3.43e-07	1.40e-06	**1.26e-06**	**2.72e-07**	3.99e-07
n	**0.0361**	0.0642	0.3659	**0.3383**	**0.0317**	0.0833

ence technique: Initial pilot study," *IEEE International Ultrasonics Symposium (IUS)*, pp. 1–4, 2017.

[2] K. B. Raja, M. Madheswaran, and K. Thyagarajah, "Ultrasound kidney image analysis for computerized disorder identification and classification using content descriptive power spectral features," *Journal of Medical Systems*, vol. 31, pp. 307317, 2007.

[3] A. Coila et al, "In vivo attenuation estimation in human thyroid nodules using the regularized spectral log difference technique: Initial pilot study," *IEEE International Ultrasonics Symposium (IUS)*, pp. 1–4, 2017.

[4] B. L. McFarlin, V. Kumar, T. A. Bigelow, D. G. Simpson, R. C. White-Traut, J. S. Abramowicz, and W. D. O'Brien Jr, "Beyond cervical length: A pilot study of ultrasonic attenuation for early detection of preterm birth risk," *Ultrasound in Medicine Biology*, vol. 41, pp. 3023–3029, 2015.

[5] A. Coila, G. Torres, J. Rouyer, S. Aristizabal, M. Urban, and R. Lavarello, "Recent developments in spectral-based ultrasonic tissue characterization," *International Symposium on Biomedical Imaging (ISBI)*, 2018.

[6] A. L. Coila and R. Lavarello, "Regularized spectral log difference technique for ultrasonic attenuation imaging," *IEEE Transactions on Ultrasonics, Ferroelectrics, and Frequency Control*, vol. 65, March 2018.

[7] Z. Vajihi, I.R. Mendez, T.J. Hall, and H. Rivaz, "Low variance estimation of backscatter quantitative ultrasound parameters using dynamic programming," *IEEE Transactions on Ultrasonics, Ferroelectrics, and Frequency Control*, September 2018.

[8] K. Nam, J. A. Zagzebski, and T. J. Hall, "Simultaneous backscatter and attenuation estimation using a least squares method with constraints," *Ultrasound in medicine & biology*, vol. 37, no. 12, pp. 2096–2104, 2011.

[9] Ivan M Rosado-Mendez, Kibo Nam, Timothy J Hall, and James A Zagzebski, "Task-oriented comparison of power spectral density estimation methods for quantifying acoustic attenuation in diagnostic ultrasound using a reference phantom method," *Ultrasonic imaging*, vol. 35, no. 3, pp. 214–234, 2013.